

# Use of Harmonic Decomposition Models in Rotorcraft Flight Control Design with Alleviation of Vibratory Loads

Umberto Saetti  
PhD Candidate

Department of Aerospace Engineering  
The Pennsylvania State University  
University Park, PA 16802

Joseph F. Horn  
Professor

Department of Aerospace Engineering  
The Pennsylvania State University  
University Park, PA 16802

**Abstract**—An Explicit Model Following (EMF) control scheme is designed to achieve stability and desired Rate Command / Attitude Hold (RCAH) response around the roll, pitch and yaw axes, while alleviating vibratory loads through both feed-forward and feedback compensation. First, the effect of command model tailoring is explored to understand the effect of feed-forward compensation on vibratory loads, with a focus on the main rotor pitch links. Secondly, the harmonic decomposition methodology is extended to enable optimization of primary flight control laws that mitigate vibratory loads. Specifically, Linear Time Periodic (LTP) systems representative of the periodic rotorcraft dynamics are approximated by Linear Time Invariant (LTI) models, which are then reduced and used in LQR design to constrain the harmonics of the vibratory loads. The gains derived are incorporated in the EMF scheme for feedback compensation. Finally, simulation results with and without load alleviation are compared and the impact of feed-forward and feedback compensation on handling qualities is assessed in terms of ADS-33E specifications.

## I. INTRODUCTION

The benefits of load alleviation control and envelope cueing have been demonstrated in numerous simulation studies [1], [2], [3], [4], [5], [6]. The use of Automatic Flight Control System (AFCS) or active control sticks to help the pilot observe structural constraints can extend the life of critical dynamic components and reduce cost of operation. These technologies can also improve handling qualities by alleviating pilot workload associated with monitoring envelope limits. Load alleviating controls have been implemented on the V-22 tilt-rotor aircraft, using cyclic pitch control to reduce in-plane loads during forward flight maneuvers [7].

Many of the critical structural limits on rotorcraft are associated with vibratory loads and fatigue limits. These loads are strongly influenced by higher harmonic (greater than 1/rev) dynamics in the rotor systems. These dynamics are not modelled in the Linear Time Invariant (LTI) dynamic models normally used for rotorcraft primary flight control design. Past work in the design of load limiting control laws has used proxy models of the vibratory loading. An example is the Equivalent Retreating Indicated Tip Speed (ERITS) parameter, which has been correlated with vibratory pitch link loads that occur with retreating blade stall onset [8]. Vibratory load limiting has also been demonstrated using basic correlations, curve

fits, or neural network approximations of vibratory loads as a function of aircraft states (angular rates, accelerations, load factor, airspeed) [1], [2], [3].

Reliance on non-physics-based models and curve fits to approximate vibratory loads is a limitation of past work. On the other hand, Linear Time Periodic (LTP) models are well-suited for representing vibratory loads on rotorcraft, including the dominant Nb/rev vibratory forces and moments at the hub and associated dynamic components, and they can be derived directly from the physics-based models. Recently, methods have been developed for approximating LTP systems using high order LTI models [9], [10]. The harmonic decomposition method transforms higher frequency harmonics into states of an LTI state space model. Harmonic decomposition methods have been used to model interactions between Higher Harmonic Control (HHC) systems and the primary Automatic Flight Control System (AFCS) and to optimize the design of these systems to reduce vibration and provide stability and handling qualities augmentation, where the HHC is primary responsible for vibratory load reduction.

While the use of harmonic decomposition method for HHC/AFCS design has been well-studied, the method has not yet been applied towards design of load alleviation control and cueing methods that act solely through the primary flight controls (1st harmonic swashplate control) and AFCS. Previous studies have shown that tailoring of response characteristics through limiting or modification of response bandwidth can significantly reduce vibratory loads, and could be significantly cheaper to implement on existing rotorcraft. The objective of this research is to extend the harmonic decomposition methodology to enable optimization of primary flight control laws that alleviate vibratory loads while meeting desired handling qualities. The use of high order LTI models is used to derive correlations of the controlled aircraft states to main rotor vibratory loads directly from the linearized physics model. In particular, the high order LTI models are reduced and used to design an EMF controller with LQR feedback optimized to reduce changes in vibratory loads.

## II. HIGH ORDER LTI MODEL EXTRACTION

### A. Nonlinear Model

This investigation uses a FLIGHTLAB<sup>®</sup> model of a notional conventional utility helicopter representative of a UH-60, as shown in Fig. 1. The model includes flexible blades with representative in-plane, out-of-plane, and torsional bending modes, in addition to the rigid blade flap and lag dynamics. A six-state Peters-He inflow model is utilized and complete nonlinear aerodynamic look-up tables are used for airframe and rotor blade aerodynamic coefficients. The model is described in further detail in [1].



Fig. 1: UH-60 helicopter.

### B. Linearization Procedure

The following procedure is similar to the one found in [11] but focuses on a first order formulation of a LTP. Consider a nonlinear system of the form

$$\dot{\mathbf{x}} = \mathbf{f}(\mathbf{x}, \dot{\mathbf{x}}, \mathbf{u}) \quad (1a)$$

$$\mathbf{y} = \mathbf{g}(\mathbf{x}, \dot{\mathbf{x}}, \mathbf{u}) \quad (1b)$$

where  $\mathbf{x}$  is the state vector of dimension  $n$ ,  $\mathbf{u}$  is the control vector of dimension  $m$ , and  $\mathbf{y}$  is the output vector of dimension  $l$ . Considering now consider the case of small disturbances

$$\mathbf{x} = \mathbf{x}_e(\psi) + \Delta\mathbf{x} \quad (2a)$$

$$\mathbf{u} = \mathbf{u}_e(\psi) + \Delta\mathbf{u} \quad (2b)$$

$$\mathbf{y} = \mathbf{y}_e(\psi) + \Delta\mathbf{y} \quad (2c)$$

where  $\mathbf{x}_e(\psi)$ ,  $\mathbf{y}_e(\psi)$ , and  $\mathbf{u}_e(\psi)$  define a periodic equilibrium condition

$$\dot{\mathbf{x}}_e = \mathbf{f}(\mathbf{x}_e, \dot{\mathbf{x}}_e, \mathbf{u}_e) \quad (3a)$$

$$\mathbf{y}_e = \mathbf{g}(\mathbf{x}_e, \dot{\mathbf{x}}_e, \mathbf{u}_e) \quad (3b)$$

A Taylor series expansion can now be performed on the state vector time derivative. After neglecting the terms of second order and higher the following equation is derived

$$\mathbf{f}(\mathbf{x}_e + \Delta\mathbf{x}, \dot{\mathbf{x}}_e + \Delta\dot{\mathbf{x}}, \mathbf{u}_e + \Delta\mathbf{u}) = \mathbf{f}(\mathbf{x}_e, \dot{\mathbf{x}}_e, \mathbf{u}_e) + \mathbf{F}(\psi)\Delta\mathbf{x} + \mathbf{K}(\psi)\Delta\dot{\mathbf{x}} + \mathbf{G}(\psi)\Delta\mathbf{u} \quad (4)$$

where

$$\mathbf{F}(\psi) = \left. \frac{\partial \mathbf{f}(\mathbf{x}, \dot{\mathbf{x}}, \mathbf{u})}{\partial \mathbf{x}} \right|_{\mathbf{x}_e, \dot{\mathbf{x}}_e, \mathbf{u}_e} \quad (5a)$$

$$\mathbf{K}(\psi) = \left. \frac{\partial \mathbf{f}(\mathbf{x}, \dot{\mathbf{x}}, \mathbf{u})}{\partial \dot{\mathbf{x}}} \right|_{\mathbf{x}_e, \dot{\mathbf{x}}_e, \mathbf{u}_e} \quad (5b)$$

$$\mathbf{G}(\psi) = \left. \frac{\partial \mathbf{f}(\mathbf{x}, \dot{\mathbf{x}}, \mathbf{u})}{\partial \mathbf{u}} \right|_{\mathbf{x}_e, \dot{\mathbf{x}}_e, \mathbf{u}_e} \quad (5c)$$

With a few steps of algebraic manipulation, one can derive

$$\Delta\dot{\mathbf{x}} = \hat{\mathbf{F}}(\psi)\Delta\mathbf{x} + \hat{\mathbf{G}}(\psi)\Delta\mathbf{u} \quad (6)$$

where

$$\hat{\mathbf{F}}(\psi) = (\mathbf{I} - \mathbf{K})^{-1} \mathbf{F} \quad (7a)$$

$$\hat{\mathbf{G}}(\psi) = (\mathbf{I} - \mathbf{K})^{-1} \mathbf{G} \quad (7b)$$

A Taylor series expansion can be performed also on the output. After neglecting the terms of second order and higher the following equation is derived

$$\mathbf{g}(\mathbf{x}_e + \Delta\mathbf{x}, \dot{\mathbf{x}}_e + \Delta\dot{\mathbf{x}}, \mathbf{u}_e + \Delta\mathbf{u}) = \mathbf{g}(\mathbf{x}_e, \dot{\mathbf{x}}_e, \mathbf{u}_e) + \mathbf{P}(\psi)\Delta\mathbf{x} + \mathbf{Q}(\psi)\Delta\dot{\mathbf{x}} + \mathbf{R}(\psi)\Delta\mathbf{u} \quad (8)$$

where

$$\mathbf{P}(\psi) = \left. \frac{\partial \mathbf{g}(\mathbf{x}, \dot{\mathbf{x}}, \mathbf{u})}{\partial \mathbf{x}} \right|_{\mathbf{x}_e, \dot{\mathbf{x}}_e, \mathbf{u}_e} \quad (9a)$$

$$\mathbf{Q}(\psi) = \left. \frac{\partial \mathbf{g}(\mathbf{x}, \dot{\mathbf{x}}, \mathbf{u})}{\partial \dot{\mathbf{x}}} \right|_{\mathbf{x}_e, \dot{\mathbf{x}}_e, \mathbf{u}_e} \quad (9b)$$

$$\mathbf{R}(\psi) = \left. \frac{\partial \mathbf{g}(\mathbf{x}, \dot{\mathbf{x}}, \mathbf{u})}{\partial \mathbf{u}} \right|_{\mathbf{x}_e, \dot{\mathbf{x}}_e, \mathbf{u}_e} \quad (9c)$$

After substituting 6 in 8 and carrying on the calculations, one can derive

$$\Delta\mathbf{y} = \hat{\mathbf{P}}(\psi)\Delta\mathbf{x} + \hat{\mathbf{R}}(\psi)\Delta\mathbf{u} \quad (10)$$

where

$$\hat{\mathbf{P}}(\psi) = \mathbf{P} + \mathbf{Q}\hat{\mathbf{F}} \quad (11a)$$

$$\hat{\mathbf{R}}(\psi) = \mathbf{R} + \mathbf{Q}\hat{\mathbf{G}} \quad (11b)$$

It is thus obtained a first order formulation of a LTP system representative of the periodic rotorcraft dynamics.

In practice, the nonlinear FLIGHTLAB<sup>®</sup> model is first trimmed at a desired flight condition. Then a nonlinear simulation is run until the azimuthal position of a reference blade reaches  $\psi = 0^\circ$ . Finally, the model is linearized at incremental azimuth positions over one rotor revolution. In the present study the flight condition is chosen to be level flight at 120 knots and the time step to be  $\Delta\psi = 0.5^\circ$ , which gives a total of 720 azimuthal positions.

The notation is simplified by dropping the  $\Delta$  in front of the linearized variables, remembering that they are indeed perturbations from a periodic equilibrium. The state, input, and output vectors of the LTP system are given by

$$\mathbf{x}^T = [\mathbf{x}_B^T \ \mathbf{x}_R^T] \quad (12a)$$

$$\mathbf{u}^T = [\delta_{lat} \ \delta_{long} \ \delta_{ped}] \quad (12b)$$

$$\mathbf{y}^T = [\mathbf{x}_B^T \ \mathbf{F}_{PL}^T] \quad (12c)$$

where the subscript  $( )_B$  indicates the rigid body states and  $( )_R$  denotes the states relative to the rotor dynamics.  $\mathbf{F}_{PL}$  is

the vector of forces acting on a reference pitch link. The rigid body state vector is given by, in order, the body velocities  $u, v, w$ , the body angular rates  $p, q, r$ , and the Euler angles  $\phi, \theta, \psi$ . The rotor states include inflow, rigid flap, lag and torsion in Multiple Blade Coordinates (MBC), the slowest 11 bending modes also in MBC, and the time derivatives of all the variables in MBC. The system has a total of  $n = 116$  states,  $m = 3$  inputs, and  $l = 12$  outputs.

### C. Harmonic Decomposition

The state, input, and output of the LTP system obtained above are decomposed into a finite number of harmonics via Fourier analysis.

$$\mathbf{x} = \mathbf{x}_0 + \sum_{i=1}^N \mathbf{x}_{ic} \cos i\psi + \mathbf{x}_{is} \sin i\psi \quad (13a)$$

$$\mathbf{u} = \mathbf{u}_0 \quad (13b)$$

$$\mathbf{y} = \mathbf{y}_0 + \sum_{j=1}^L \mathbf{y}_{jc} \cos j\psi + \mathbf{y}_{js} \sin j\psi \quad (13c)$$

Note that only the 0<sup>th</sup> harmonic of the input vector is retained. This is because the present study considers solely primary flight control actuation, thus disregarding any sort of higher harmonic control. In fact, the desired maximum frequency of the control signal is significantly less than the main rotor angular speed. As it is shown in [9], the LTP model can be transformed into an approximate high order LTI model

$$\dot{\mathbf{X}} = \mathbf{A}\mathbf{X} + \mathbf{B}\mathbf{U} \quad (14a)$$

$$\mathbf{Y} = \mathbf{C}\mathbf{X} + \mathbf{D}\mathbf{U} \quad (14b)$$

where

$$\mathbf{X}^T = [\mathbf{x}_0^T \mathbf{x}_{1s}^T \mathbf{x}_{1c}^T \cdots \mathbf{x}_{Ns}^T \mathbf{x}_{Nc}^T] \quad (15a)$$

$$\mathbf{U} = \mathbf{u}_0 \quad (15b)$$

$$\mathbf{Y}^T = [\mathbf{y}_0^T \mathbf{y}_{1s}^T \mathbf{y}_{1c}^T \cdots \mathbf{y}_{Ls}^T \mathbf{y}_{Lc}^T] \quad (15c)$$

are respectively the augmented state, control, and output vectors.

In the present study the number of harmonics retained for the state and the output is  $N = L = 4$ , leading to a high order LTI system with  $n(2N + 1) = 1044$  states, 4 inputs, and  $l(2L + 1) = 108$  outputs. The state, input and output vectors of the high order LTI system are given by

$$\mathbf{X}^T = [\mathbf{x}_{B_0}^T \mathbf{x}_{R_0}^T \mathbf{x}_{B_{1s}}^T \mathbf{x}_{R_{1s}}^T \cdots \mathbf{x}_{B_{4c}}^T \mathbf{x}_{R_{4c}}^T] \quad (16a)$$

$$\mathbf{U} = [\delta_{lat_0} \delta_{lon_0} \delta_{ped_0}] \quad (16b)$$

$$\mathbf{Y}^T = [\mathbf{x}_{B_0}^T \mathbf{F}_{PL_0}^T \mathbf{x}_{B_{1s}}^T \mathbf{F}_{PL_{1s}}^T \cdots \mathbf{x}_{B_{4c}}^T \mathbf{F}_{PL_{4c}}^T] \quad (16c)$$

## III. CONTROLLER DESIGN

A controller is designed to achieve stability and desired RCAH response around the roll, pitch and yaw axes, while alleviating unsteady loads during maneuver with only conventional primary control. This restricts the maximum allowable frequency of the input to be considerably less than the main rotor angular speed, excluding any higher harmonic control. Note that the collective stick, which is usually used to mainly control altitude, is left open-loop.

### A. Reduced-Order Models

Due to the fact that low order models make the control design more tractable, and because of the difficulty of measuring or estimating the states associated with flapping and inflow dynamics, this research proposes a reduced order model approach to feedback control design. The problem is addressed through residualization, a method based on singular perturbation theory [12] that accurately models low frequency and steady state but neglects high frequency. It assumes that the ‘‘fast’’ states reach steady state more quickly than the ‘‘slow’’ states. The state vector is hence divided into fast and slow components:

$$\mathbf{X} = \begin{bmatrix} \mathbf{X}_s \\ \mathbf{X}_f \end{bmatrix} \quad (17)$$

where

$$\mathbf{X}_s = \mathbf{x}_{B_0} \quad (18)$$

$$\mathbf{X}_f^T = [\mathbf{x}_{R_0}^T \mathbf{x}_{B_{1s}}^T \mathbf{x}_{R_{1s}}^T \cdots \mathbf{x}_{B_{4c}}^T \mathbf{x}_{R_{4c}}^T] \quad (19)$$

The dynamical system can then be re-written in the following form

$$\begin{bmatrix} \dot{\mathbf{X}}_s \\ \dot{\mathbf{X}}_f \end{bmatrix} = \begin{bmatrix} \mathbf{A}_s & \mathbf{A}_{sf} \\ \mathbf{A}_{fs} & \mathbf{A}_f \end{bmatrix} \begin{bmatrix} \mathbf{X}_s \\ \mathbf{X}_f \end{bmatrix} + \begin{bmatrix} \mathbf{B}_s \\ \mathbf{B}_f \end{bmatrix} \mathbf{U} \quad (20)$$

By assuming that the fast states reach steady state quickly, the algebraic constraint  $\dot{\mathbf{x}}_f = 0$  can be imposed. It follows that

$$\mathbf{A}_{fs}\mathbf{X}_s + \mathbf{A}_f\mathbf{X}_f + \mathbf{B}_f\mathbf{U} = 0 \quad (21)$$

Solving for the fast states leads to

$$\mathbf{X}_f = \mathbf{A}_f^{-1}(-\mathbf{A}_{fs}\mathbf{X}_s - \mathbf{B}_f\mathbf{U}) \quad (22)$$

By substituting the latter result into 20, a new expression for the slow states can be found

$$\dot{\mathbf{X}}_s = \hat{\mathbf{A}}\mathbf{X}_s + \hat{\mathbf{B}}\mathbf{U} \quad (23)$$

where

$$\hat{\mathbf{A}} = \mathbf{A}_s - \mathbf{A}_{sf}\mathbf{A}_f^{-1}\mathbf{A}_{fs} \quad (24a)$$

$$\hat{\mathbf{B}} = \mathbf{B}_s - \mathbf{A}_{sf}\mathbf{A}_f^{-1}\mathbf{B}_f \quad (24b)$$

Considering now the output equation

$$\mathbf{Y} = [\mathbf{C}_s \quad \mathbf{C}_f] \begin{bmatrix} \mathbf{X}_s \\ \mathbf{X}_f \end{bmatrix} + \mathbf{D}\mathbf{u} \quad (25)$$

and by substituting 22 in it, one can derive

$$\mathbf{Y} = \hat{\mathbf{C}}\mathbf{X}_s + \hat{\mathbf{D}}\mathbf{U} \quad (26)$$

where

$$\hat{\mathbf{C}} = \mathbf{C}_s - \mathbf{C}_f\mathbf{A}_f^{-1}\mathbf{A}_{fs} \quad (27a)$$

$$\hat{\mathbf{D}} = \mathbf{D} - \mathbf{C}_f\mathbf{A}_f^{-1}\mathbf{B}_f \quad (27b)$$

Now, since the higher order harmonics of the rigid body states are impractical to observe and, in general, of negligible amplitude when compared to their respective 0<sup>th</sup> harmonic, they are truncated from the output (meaning also from  $\hat{\mathbf{C}}$  and  $\hat{\mathbf{D}}$ ). The output therefore reduces to

$$\mathbf{Y}^T = [\mathbf{x}_{B_0}^T \mathbf{F}_{PL_0}^T \mathbf{F}_{PL_{1s}}^T \mathbf{F}_{PL_{1c}}^T \cdots \mathbf{F}_{PL_{4c}}^T] \quad (28)$$

where  $\mathbf{F}_{PL}$  denotes the pitch link load vector. The idea is to predict the vibratory loads with sufficient accuracy using

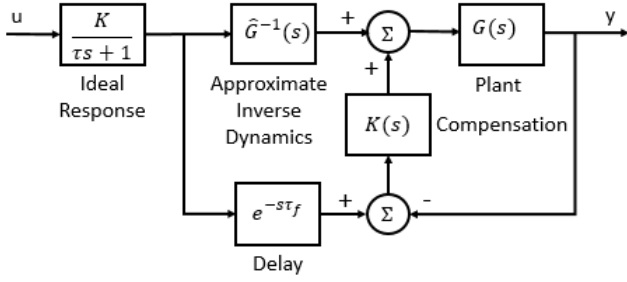


Fig. 2: Explicit model following block diagram.

the 9<sup>th</sup> order approximation of the high order LTI model just derived. Note that all of the higher harmonics of the pitch link loads are kept in the output to capture the dependence of controls and rigid body states on the vibratory loads. This model is used in the feedback design of the EMF controller presented in the next section.

An 11<sup>th</sup> order model is also derived in a similar fashion. The 0<sup>th</sup> harmonic of the longitudinal and lateral flapping is retained in the slow state, along with the rigid body states. Since this model is only used to extract time delay parameters used in the feed-forward design of the EMF controller, there is no need for it to predict the vibratory loads. Hence, the harmonics higher than the 0<sup>th</sup> are truncated and the slow and fast components of the state vector are selected from the averaged model as follows

$$\mathbf{X}_s^T = [\mathbf{x}_{B_0}^T \ \beta_{1s_0} \ \beta_{1c_0}] \quad (29a)$$

$$\mathbf{X}_f = \hat{\mathbf{x}}_{R_0} \quad (29b)$$

where  $\hat{\mathbf{x}}_{R_0}$  denotes the vector of the 0<sup>th</sup> harmonic rotor states deprived of longitudinal and lateral flapping.

### B. Explicit Model Following

A general EMF scheme for a SISO system is shown in Fig. 2. The present study does not assume perfect inverse plant dynamics, in fact the inverse plant is based on a set of decoupled 1<sup>st</sup> order linear models, where the stability and control derivatives are pulled from the 9<sup>th</sup> order model. Specifically, the inverse plant on the roll, pitch, and yaw axes is approximated respectively by the following inverse transfer functions

$$\frac{\delta_{lat}}{p} = \frac{s - L_p}{L_{\delta_{lat}}} \quad (30a)$$

$$\frac{\delta_{long}}{q} = \frac{s - M_q}{M_{\delta_{long}}} \quad (30b)$$

$$\frac{\delta_{ped}}{r} = \frac{s - N_r}{N_{\delta_{ped}}} \quad (30c)$$

The stability derivatives  $L_p$ ,  $M_q$ , and  $N_r$  are obtained from the following portion of the 9<sup>th</sup> order model system matrix, as in 31,

$$\dot{\begin{bmatrix} p \\ q \\ r \end{bmatrix}} = \begin{bmatrix} L_p & \cdot & \cdot \\ \cdot & M_q & \cdot \\ \cdot & \cdot & N_r \end{bmatrix} \begin{bmatrix} p \\ q \\ r \end{bmatrix} \quad (31)$$

whereas control derivatives  $L_{\delta_{lat}}$ ,  $M_{\delta_{long}}$  and  $N_{\delta_{ped}}$  are obtained from the input matrix of the 9<sup>th</sup> order model, as shown in 32.

$$\dot{\begin{bmatrix} \delta_{lat} \\ \delta_{long} \\ \delta_{ped} \end{bmatrix}} = \begin{bmatrix} L_{\delta_{lat}} & \cdot & \cdot \\ \cdot & M_{\delta_{long}} & \cdot \\ \cdot & \cdot & N_{\delta_{ped}} \end{bmatrix} \begin{bmatrix} \delta_{lat} \\ \delta_{long} \\ \delta_{ped} \end{bmatrix} \quad (32)$$

The present study utilizes a Linear Quadratic regulator (LQR) both for disturbance rejection and to pursue load alleviation. Fig. 3 shows the practical implementation of LQR in the EMF design. The turn coordination block is explained in detail in [1]. The equivalent rotor delay time constant  $\tau_f$ , used to delay the ideal response such that it can be physically followed by the controlled system, is taken as  $\max\{\tau_{f_{1c}}, \tau_{f_{1s}}\}$ , where  $\tau_{f_{1c}}$  and  $\tau_{f_{1s}}$  are extracted from the portion of the system matrix of the 11<sup>th</sup> order model, as shown in 33.

$$\dot{\begin{bmatrix} \beta_{1c} \\ \beta_{1s} \end{bmatrix}} = \begin{bmatrix} \beta_{1c} & \beta_{1a} \\ -\frac{1}{\tau_{f_{1c}}} & \cdot \\ \cdot & -\frac{1}{\tau_{f_{1s}}} \end{bmatrix} \begin{bmatrix} \beta_{1c} \\ \beta_{1s} \end{bmatrix} \quad (33)$$

Note that the gains  $K_p$ ,  $K_q$  and  $K_r$  relate each pilot input to the respective commanded angular rate whereas the time constants  $\tau_p$ ,  $\tau_q$  and  $\tau_r$  determine the quickness of the ideal response on each axis.

### C. LQR Design

Since the loop on the right hand side of Fig. 2 is independent from the the inverse plant, the LQR gains can be determined by using the 9<sup>th</sup> order model previously derived. The idea is to minimize a cost function that takes into account the output, such as

$$J = \int_0^t [\mathbf{Y}^T \hat{\mathbf{Q}} \mathbf{Y} + \mathbf{U}^T \hat{\mathbf{R}} \mathbf{U}] d\tau \quad (34)$$

The state cost can be restored by substituting the output equation of the reduced order system in Eq. 34, obtaining

$$J = \int_0^t [\mathbf{X}_s^T \mathbf{Q} \mathbf{X}_s + \mathbf{U}^T \mathbf{R} \mathbf{U}] d\tau \quad (35)$$

where the state and control cost matrices are defined as

$$\mathbf{Q} = \hat{\mathbf{C}}^T \hat{\mathbf{Q}} \hat{\mathbf{C}} \quad (36a)$$

$$\mathbf{R} = \hat{\mathbf{D}} + \hat{\mathbf{D}}^T \hat{\mathbf{Q}} \hat{\mathbf{D}} \quad (36b)$$

The weight matrices are designed according to [13] and are of the form of

$$\hat{\mathbf{Q}} = \text{diag} \left[ \frac{\alpha_1^2}{(Y_1)_{max}^2} \ \frac{\alpha_2^2}{(Y_2)_{max}^2} \ \cdots \ \frac{\alpha_n^2}{(Y_n)_{max}^2} \right] \quad (37)$$

$$\hat{\mathbf{R}} = \rho \text{diag} \left[ \frac{\beta_1^2}{(U_1)_{max}^2} \ \frac{\beta_2^2}{(U_2)_{max}^2} \ \cdots \ \frac{\beta_m^2}{(U_m)_{max}^2} \right] \quad (38)$$

where  $(Y_i)_{max}^2$  and  $(U_j)_{max}^2$  are the largest desired response and input for that particular component of the output/input,  $\sum_{i=1}^l \alpha_i^2 = 1$  and  $\sum_{j=1}^m \beta_j^2 = 1$  are used to add an additional relative weighting on the various components of the output/control input, and  $\rho$  is used as the relative weighting between the control and state penalties.

The method described allows to transfer the constraints on each harmonic of the pitch link load response to the fuselage

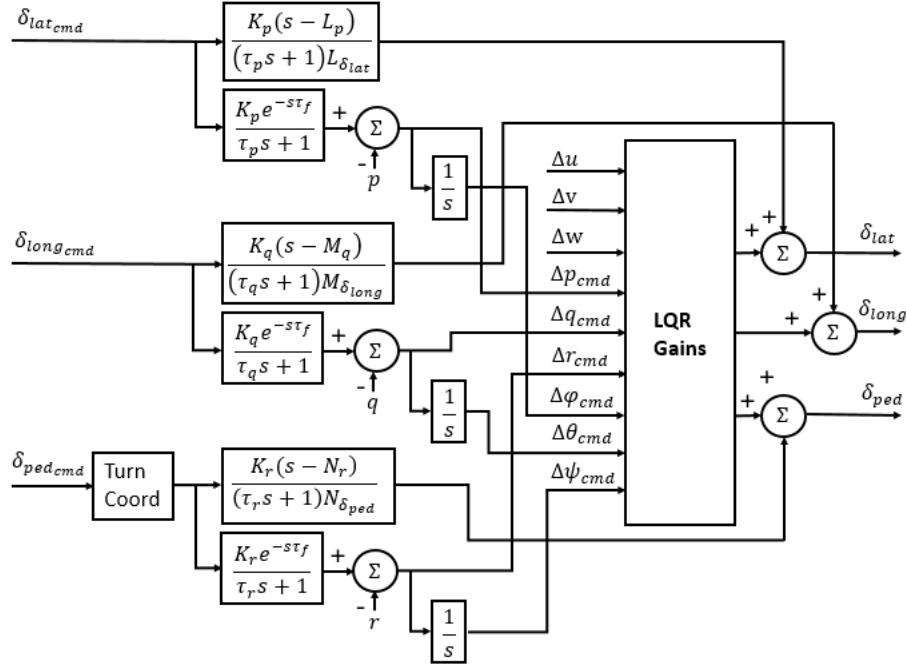


Fig. 3: Explicit model following block diagram with LQR disturbance rejection.

states, effectively providing a load limiting control action based on the feedback of the 0<sup>th</sup> harmonic fuselage dynamics. Note that what is actually being minimized is the perturbations of pitch link loads from their periodic equilibrium. This means that the controller tends to bring the pitch link loads to their periodic equilibrium. It follows that the load alleviating action is effective only in maneuvering flight.

#### IV. RESULTS

##### A. Correlation of Vibratory Loads to Response Bandwidth

In preliminary studies the effect of command model tailoring is explored to understand its impact on vibratory loads, with focus on the main rotor pitch links. Initial simulation studies illustrate the correlation of vibratory loads to response bandwidth. The selected flight condition is level flight at 120 kts. To study the effects of roll rate and roll acceleration on the vibratory loads independently, the roll controller has been set up as a rate command (RCAH) system. This way, roll acceleration due to a step input can be modified by acting on the time constant of the first order command filter while keeping the magnitude of the roll rate perturbation constant. Note that the roll acceleration is equivalent to the natural frequency of the command filter, which is the inverse of the time constant:  $\omega_n = \frac{1}{\tau}$ . The LQR gains are found by imposing constraints only on the fuselage states.

Fig. 4 shows a roll rate doublet response for varying natural frequencies. Fig. 5 shows the correlation between pitch link loads and roll rates for different roll accelerations, given by the different natural frequencies of the rate command filter. It appears that increasing roll accelerations has a greater effect on pitch link loads for higher roll rates. It is concluded that command model tailoring does indeed have an effect on vibratory loads and is a viable way to load alleviation.

Nonetheless, it comes at the cost of performance since the agility of the rotorcraft decreases with decreasing command filter natural frequencies.

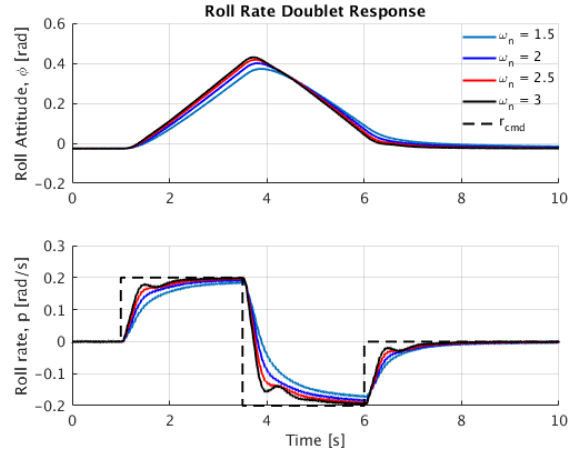


Fig. 4: Roll attitude and roll rate time response in RCAH mode with varying natural frequencies.

##### B. Validation of the Linear Models

The open-loop response of the linear models is compared to the open-loop response of the nonlinear system to ensure that both the fuselage dynamics and the vibratory loads are accurately modeled. The rate command time history of the maneuver in consideration is the same as Fig. 4. The attitude and angular rates from the simulations are shown respectively in Fig. 6 and 7. As it appears in the plots, the LTP model response overlaps the one of the LTI system for each fuselage output. Both the high order LTI and LTP on-axis responses

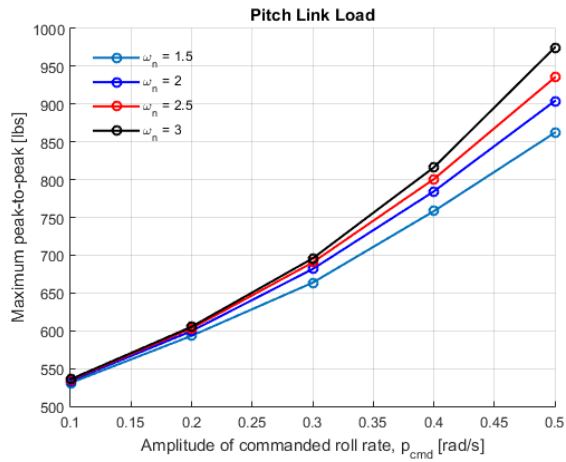


Fig. 5: Maximum peak-to-peak pitch link load with varying roll rate command filter natural frequencies.

match the nonlinear response well. The off-axis responses seem to give a good match in yaw, less in pitch. The reduced order LTI response is very similar to the high order LTI one. The only noticeable difference is that the high order LTI system contains a model of the actuators acting on the swashplate, of which the states are lost during reduction. This causes the roll response not to have a delay, as it can be appreciated in the angular rates plot. The vibratory response of the z-component of a reference pitch link load and its perturbation from the periodic equilibrium are shown respectively in Fig. 8 and Fig. 9. Mind that the linear responses in the plots have the periodic equilibrium added in to facilitate the comparison with the nonlinear response. All the linear models seem to predict the peaks and harmonic content of the vibratory loads accurately.

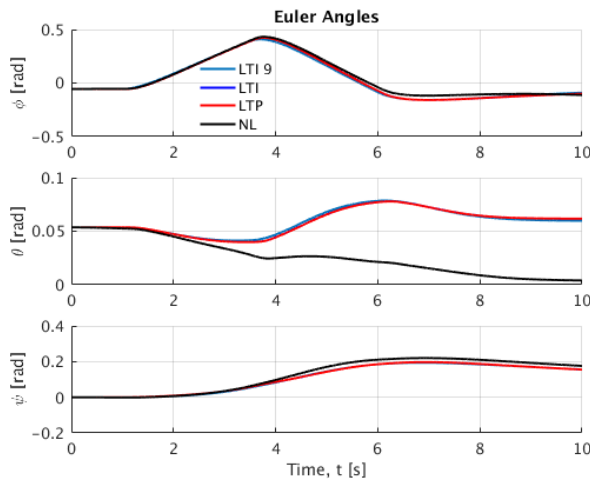


Fig. 6: Attitude time history of the reduced order, high order LTI, LTP and nonlinear models.

The fidelity of the reduced order model is also assessed by comparing its eigenvalues to the ones of the high order LTI system, as shown in Fig. 10. As expected, the rigid body eigenvalues of the reduced order model match closely to the

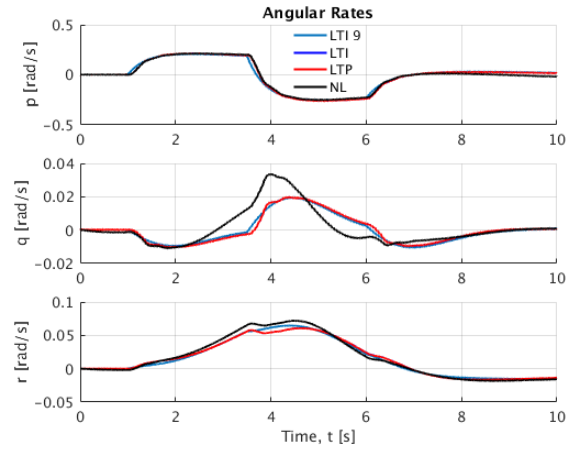


Fig. 7: Angular rates time history of the reduced order, high order LTI, LTP and nonlinear models.

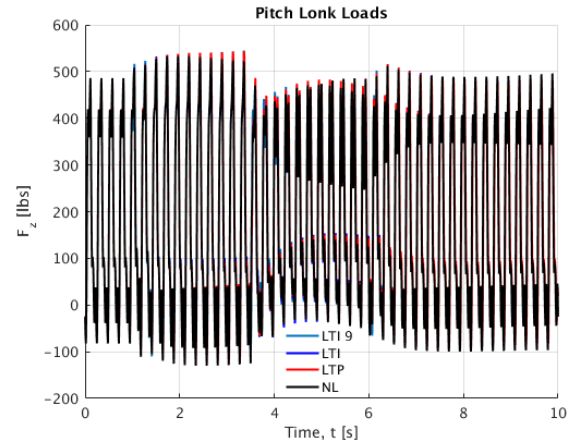


Fig. 8: Pitch link load z-component time history of the reduced order, high order LTI, LTP and nonlinear models.

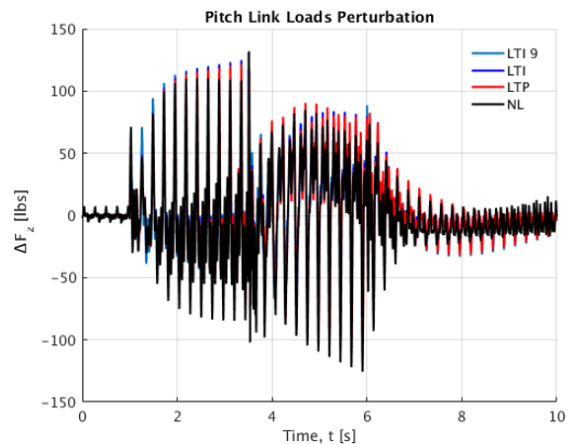


Fig. 9: Pitch link load perturbation z-component time history of the reduced order, high order LTI, LTP and nonlinear models.

ones of the high order LTI system. Fig. 11 illustrates the on-axis frequency response of the angular rates with respect to

the control inputs. It appears that up to about  $4 \text{ rad/s}$  the frequency response of the reduced order model matches closely the one of the high order LTI on each axis. It is concluded that both the fuselage dynamics and the vibratory loads are properly captured by linear systems.

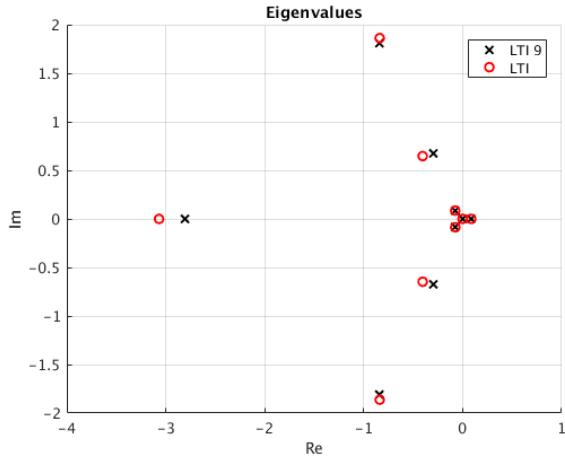


Fig. 10: Comparison between the eigenvalues of the reduced order model and high order LTI system.

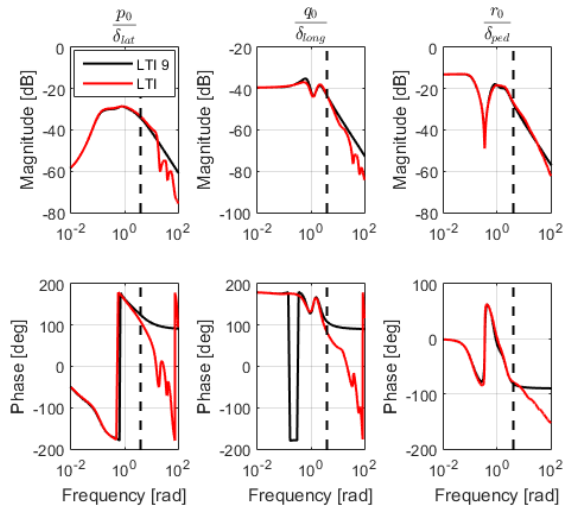


Fig. 11: Comparison between the on-axis frequency responses of the reduced order model and high order LTI system.

### C. Load Alleviating Control System

The load alleviating control system is compared to EMF with LQR disturbance rejection but no load alleviating action, which will be referred to as the baseline control system. The results of a pullup/pushover maneuver starting at 120 kts level flight are presented to understand how the load alleviation is effectively performed in terms of control actuation and rate response. The chosen roll, pitch and yaw command natural frequencies are respectively 2.5, 2.5 and  $2 \text{ rad/s}$ . The LQR gains are designed such that, following ADS-33E-PRF regulations, roll and yaw angular deviations are maintained within  $15^\circ$  from the initial unaccelerated condition. Also, the output harmonics included in the cost function are  $0^{\text{th}}$ ,  $1^{\text{st}}$  and  $4^{\text{th}}$ ; these appear

to give the best compromise between load alleviation and flight performance. The maneuver consists in a  $0.2 \text{ rad/s}$  nose-up / nose-down doublet, similar to the one in Fig. 4 but on the pitch axis. The closed-loop responses are shown in Fig. 12 and 13. The control input histories is shown in Fig. 14. Noticeably, the pitch rate response with the load alleviating control system is less aggressive and possibly slightly slower when compared to the response of the baseline controller. Furthermore, the off-axis response, specifically around the yaw axis, looks worse for the load alleviation case. Degradation in flight performance is reasonable since load alleviation is achieved solely through the  $0^{\text{th}}$  harmonic of the fuselage dynamics. To put it simply, the load alleviating control system makes the helicopter fly more “gently”. The pitch link loads and their perturbation from trim can be appreciated in Fig. 15 and Fig. 16. It is clear that the vibratory load perturbation is minimized. But the question is: how much?

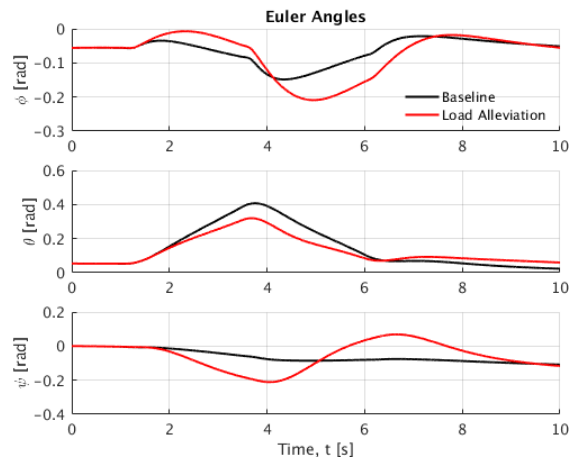


Fig. 12: Comparison between attitude time histories for baseline and load alleviating control systems.

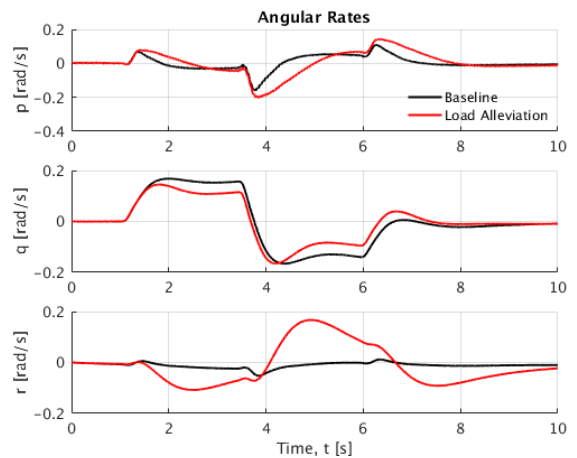


Fig. 13: Comparison between the angular rates time histories for baseline and load alleviating control systems.

The efficacy of the load alleviation control system is quantified for varying pilot input amplitudes and command

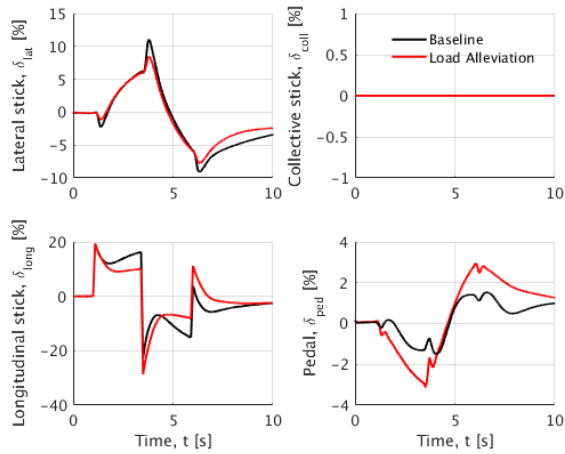


Fig. 14: Comparison between the control signals for baseline and load alleviating control systems.

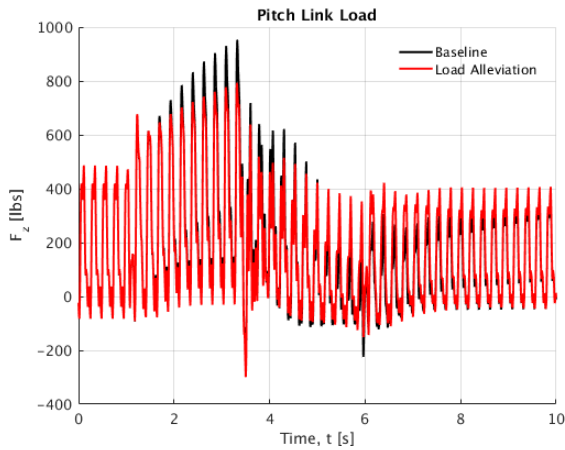


Fig. 15: Comparison between the pitch link loads for baseline and load alleviating control systems.

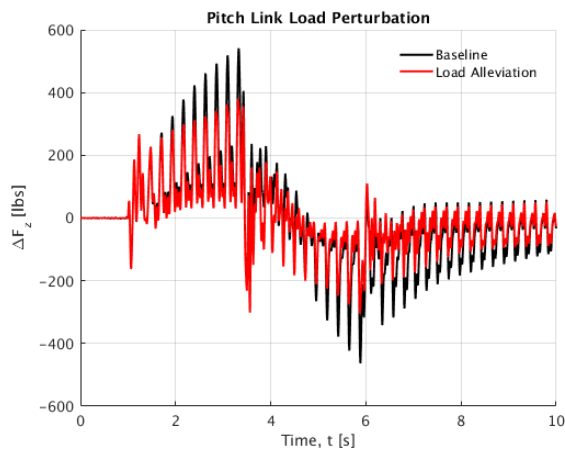


Fig. 16: Comparison between the pitch link load perturbation for baseline and load alleviating control systems.

natural frequencies, both on the roll and pitch axes. The metrics used to evaluate such efficacy are the percent reduction in Root

Mean Squared (RMS) of the pitch link load perturbations from trim and the percent reduction in maximum peak-to-peak pitch link load, with respect to the baseline control system. The representative maneuver in roll is chosen to be a roll reversal. The performance of the load alleviating controller with respect to the baseline one in terms of vibratory load mitigation is shown in Fig. 17. Although giving some improvement, the load alleviating system provides only very modest reductions in the vibratory pitch link loads in roll. However, for the pullup/pushover maneuver the percent reduction in both pitch link load perturbation RMS and maximum peak-to-peak pitch link load is more significant. Fig. 18 shows an improvement of up to 29 % of the RMS of the pitch link load perturbation at low command filter natural frequencies. It also appears that lower command natural frequencies result in higher maximum peak-to-peak percent reduction, up to around a 20 %. This is due to the fact that the part of the response where the maximum peak-to-peak occurs is dominated by the feed-forward signal and thus by command model tailoring. Decreasing the quickness of the response leaves more space for the load alleviating controller to act. Mind that it is possible that there exists a combination of output costs that leads to a better controller in terms of load alleviation; in the present study the LQR gains have been optimized manually by the authors. Numerical optimization will possibly be carried on in the future.

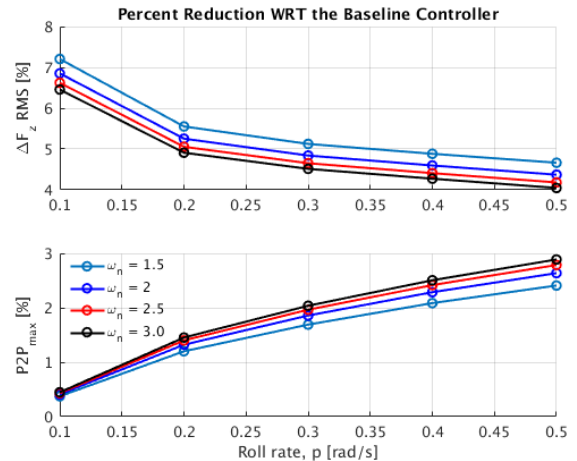


Fig. 17: Percent reduction in Root Mean Squared (RMS) of the pitch link load perturbations from trim and percent reduction in maximum peak-to-peak pitch link load for a roll reversal maneuver with load alleviation with respect to the baseline controller.

#### D. Handling Qualities Evaluation

An analysis is performed to assess the impact that the different command filter natural frequencies and the load alleviating controller have on handling qualities. Handling qualities are evaluated in terms of ADS-33E-PRF regulations for Target Acquisition and Tracking in both roll and pitch [14]. The study is based on closed-loop Simulink models, representative of the baseline and load alleviating controllers, that use the high order LTI system as plant. As shown in Fig. 19, it appears that performances degrade both with decreasing natural frequency and feedback load alleviation. Although Level 1 is not achieved in roll with the load alleviation mode

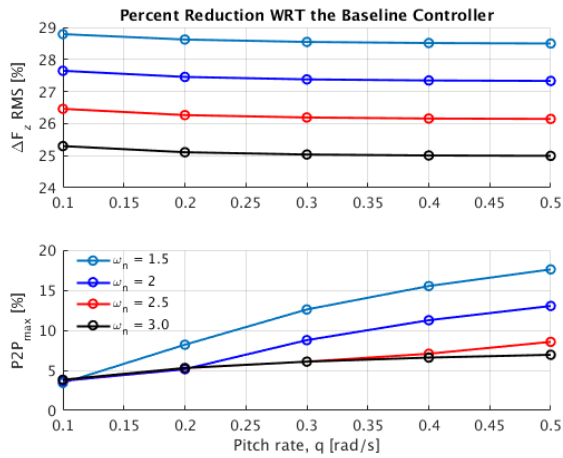


Fig. 18: Percent reduction in Root Mean Squared (RMS) of the pitch link load perturbations from trim and percent reduction in maximum peak-to-peak pitch link load for a pullup/pushover maneuver with load alleviation with respect to the baseline controller.

on, it still is met in all other Mission Task Elements (MTEs) specifications; at least for the higher command filter natural frequencies. It is concluded that load alleviation through both feed-forward and feedback compensation comes at the cost of a degradation in handling qualities.

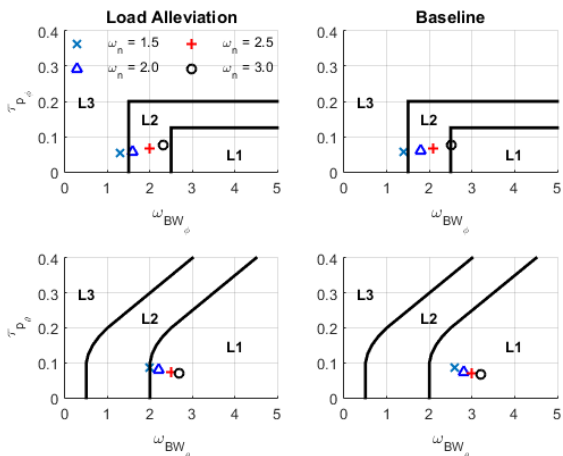


Fig. 19: Handling qualities in roll and pitch in terms of ADS-33E-PRF regulations for Targer Acquisition and Tracking, for varying command filter natural frequencies and control systems.

## V. CONCLUDING REMARKS AND FUTURE WORK

### A. Conclusion

The effect of command model tailoring is assessed to understand impact on vibratory loads. It appears that increasing roll accelerations have a greater effect on pitch link loads for higher roll rates. It is concluded that command model tailoring does indeed have an effect on vibratory loads and is a viable way to load alleviation.

A 9<sup>th</sup> order model is derived from a high order LTI system by retaining the 0<sup>th</sup> harmonic of the fuselage states and the higher harmonics of the pitch link loads in the output. The model appears to predict fuselage dynamics and vibratory loads adequately.

A controller that optimizes primary flight control laws to minimize vibratory loads is developed by incorporating LQR gains for disturbance rejection in an Explicit Model Following scheme. The gains are derived by using a reduced order model to impose constraints on the harmonics of the pitch link loads. The resulting load alleviating control action translates into a degradation of flight performance. The controller gives a good load alleviation in pullup/pushover maneuvers but appears to be less effective in a roll reversal maneuver.

Previous work limitations, such as the reliance on non-physics-based models and curve fits to approximate vibratory loads, is lifted. Since both command model tailoring and the load alleviating controller act solely through 1<sup>st</sup> harmonics of swashplate control, a combination of the two could be readily integrated with existing or future AFCS on military rotorcraft.

An analysis is performed to understand the impact that the different command filter natural frequencies and the load alleviating controller have on handling qualities. It appears that load alleviation through both feed-forward and feedback compensation comes at the cost of a degradation in handling qualities.

### B. Future Work

The present study concentrates on extracting the LTP, high order LTI and reduced order systems only at one flight condition. A goal for the near future is to derive the aforementioned models across the entire flight envelope such that the load alleviating controller can be gain-scheduled with speed. This is important since the maneuvers studied show appreciable changes in speed.

Command model and effectiveness of load alleviating action might be dependent on operating conditions, mission task, and current damage of the rotorcraft, and thus the controller will be integrated with a notional regime recognition algorithm.

The controller will be tested in piloted simulations studies to evaluate impact on handling qualities and life extension. Specifically, the incremental fatigue damage, as measured by the crack growth rate in the pitch link loads, will be assessed to understand the actual practical benefit of the method.

Control allocation methods for compound rotorcraft with redundant controls will also be explored. The harmonic decomposition LTI models will be used to develop a weighted pseudo-inverse in the control allocation that minimizes critical vibratory loads. The control allocation will adapt to mission requirements and damage state of the rotorcraft.

Rotor state feedback will be studied. The idea is to retain the 0<sup>th</sup> and possibly higher harmonics of the flapping states during reduction. The output would include all the harmonics. The resulting model would be used in the LQR gain design.

An approach where the command model and LQR gains are simultaneously tuned to meet Level 1 handling qualities while maximizing load alleviation will be considered.

## ACKNOWLEDGMENT

This research was partially funded by the Government under Agreement No. W911W6-17-2-0003. The U.S. Government is authorized to reproduce and distribute reprints for Government purposes notwithstanding any copyright notation thereon. The views and conclusions contained in this document are those of the authors and should not be interpreted as representing the official policies, either expressed or implied, of the Aviation Development Directorate or the U.S Government.

## REFERENCES

- [1] D.B. Caudle, *DAMAGE MITIGATION FOR ROTORCRAFT THROUGH LOAD ALLEVIATING CONTROL*, M.S. Thesis, The Pennsylvania State University, December 2014.
- [2] B.R. Geiger, *Flight Control Optimization on a Fully Compounded Helicopter with Redundant Control Effectors*, M.S. Thesis, The Pennsylvania State University, May 2005.
- [3] C.J. Thaiss, C.C. McColl, J. Horn, E. Keller, A. Ray, R. Semidey, and N. Phan, *Rotorcraft Real Time Load Damage Alleviation through Load Limiting Control*, AIAA/ASME/ASCE/AHS/SC Structures, Structural Dynamics, and Materials Conference, National Harbor, MD, January 13-17, 2014.
- [4] N. Sahani, and J.F. Horn, *Adaptive Model Inversion Control of a Helicopter with Structural Load Limiting*, AIAA Journal of Guidance, Control, and Dynamics, Vol. 29,(2), March-April 2006.
- [5] J.F. Horn, and N. Sahani, *Detection and Avoidance of Main Rotor Hub Moment Limits on Rotorcraft*, AIAA Journal of Aircraft, Vol. 41,(2), March-April 2004, pp. 372-379.
- [6] J.F. Horn, A.J. Calise, and J.V.R. Prasad, *Flight Envelope Limit Detection and Avoidance for Rotorcraft*, Journal of the American Helicopter Society, Vol. 47,(4), October 2002, pp. 253-262.
- [7] D.G. Miller, and N.D. Ham, *Active Control of Tilt-Rotor Blade In-Plane Loads During Maneuvers*, European Rotorcraft Forum, Milan, Italy, September 1988.
- [8] G.J. Jeram, *Open Design for Helicopter Active Control Systems*, Proceedings of the 58<sup>th</sup> Annual Forum, American Helicopter Society, Montreal, Canada, June 2002, pp. 2435-2454.
- [9] M. Lopez, and J.V.R. Prasad, *Linear Time Invariant Approximations of Linear Time Periodic Systems*, Journal of the American Helicopter Society, Vol. 62, (1), January 2017, pp. 1-10.
- [10] M. Lopez, J.V.R. Prasad, M.B. Tischler, M.D. Takahashi, and K.K. Cheung, *Simulating HHC/AFCS Interaction and Optimized Controllers using Piloted Maneuvers*, 71<sup>st</sup> Annual National Forum of the American Helicopter Society, Virginia Beach, VA, May 5-7, 2015.
- [11] J.V.R. Prasad, F.E. Olcer, L.N. Sankar, and C. He, *Linear Time Invariant Models for Integrated Flight and Rotor Control*, 35<sup>th</sup> European Rotorcraft Forum, Hamburg, Germany, September 22-25, 2009.
- [12] P.V. Kokotovic, R.E. O'Malley, and P. Sannuti, *Singular Perturbations and Order Reduction in Control Theory, an Overview*, Automatica, Vol. 12, (2), 1976, pp. 123-132.
- [13] A.E. Bryson, and Y.C. Ho, *Applied Optimal Control*, 43<sup>rd</sup> Hemisphere Publishing Corporation, Washington, D.C., 1975.
- [14] Anon, *Aeronautical Design Standard Performance Specification, Handling Qualities Requirements for Military Rotorcraft*, ADS-33-PRF, US-AAMCOM, 2000.